# Quasi-one-dimensional dipolar quantum gases

Liming Guan,[1] Xiaoling Cui,[1,2,*] Ran Qi,[3] and Hui Zhai[1,†]

[1]*Institute for Advanced Study, Tsinghua University, Beijing 100084, People's Republic of China*

[2]*Beijing National Laboratory for Condensed Matter Physics, Institute of Physics, Chinese Academy of Sciences, Beijing 100190, People's Republic of China*

[3]*School of Physics, Georgia Institute of Technology, Atlanta, Georgia 30332, USA*

(Received 9 July 2013; published 6 February 2014)

In this paper we consider dipolar quantum gases in a quasi-one-dimensional tube with dipole moment perpendicular to the tube direction. We deduce the effective one-dimensional interaction potential and show that this potential is not purely repulsive, but rather has an attractive part due to high-order scattering processes through transverse excited states. The attractive part can induce bound states and cause scattering resonances. This represents the dipole-induced resonance in low dimension. We work out an unconventional behavior of low-energy phase shift for this effective potential and show how it evolves across a resonance. Based on the phase shift, the interaction energy of spinless bosons is obtained using the asymptotic Bethe ansatz. Despite the long-range nature of dipolar interaction, we find that the behavior is similar to a short-range Lieb-Liniger gas emerging at the resonance region.

DOI: 10.1103/PhysRevA.89.023604 PACS number(s): 67.85.Jk, 03.75.Nt, 05.30.−d

## I. INTRODUCTION

Nowadays, there is a major effort in cold-atom physics to achieve degenerate gases of stable polar molecules, using stimulated Raman adiabatic passage technique [1]. Polar molecules possess a permanent electric dipole moment, which can be polarized and tuned by external electric fields. Their dipole interaction strength can be tuned as strong as comparable to or even larger than the Fermi energy of free gases or the confinement energy in a confined geometry [2]. Unlike the Coulomb or van der Waals interaction, the dipole interaction is highly anisotropic. Thus, realizing polar molecular gases provides unique many-body systems of strong and anisotropic interactions.

Since ultracold quantum gases are dilute systems, many previous studies of such systems teach us an important lesson that understanding the two-body problem is crucial for revealing properties of many-body physics. For instance, for a short-range isotropic interaction between atoms, the $1/r$ behavior of the short-range two-body wave function leads to universal Tan relations for many-body systems [3]; an understanding of confinement-induced resonance [4] is the basis for discovering the super-Tonks gas [5]. For the dipole interaction, in three-dimensional (3D) free space, the two-body problem has been solved in a number of works [6–10], which reveals a dipole-induced $s$-wave resonance (DIR). That is to say, although to the first-order Born approximation, the dipole interaction has no net effect in the $s$-wave scattering channel, the anisotropic nature of the dipole interaction allows coupling to higher partial wave channels, through which a strong effective attractive potential is generated in the $s$-wave channel. Such an attractive potential can support the bound state and cause $s$-wave scattering resonance. Benefiting from the insight of the two-body solution, intriguing properties of fermion superfluids across a DIR have been studied [11,12].

The two-body problem with dipole interaction in the confined quasi-1D system has been extensively studied in a number of previous works [13–17]. Among many of these studies a commonly used model is to take a purely attractive or repulsive potential along the 1D tube [14], as can be deduced from the lowest transverse mode approximation. However, with the experience in the 3D case, one may wonder whether this commonly used model is always valid, in particular, when the dipole interaction is strong enough to compare with the confinement energy. The studies beyond the $1/z^3$ potential include Refs. [15,16], respectively emphasizing the short-range scattering parameter modified by the dipole interaction [15] and exploring the scattering properties when the dipole moment is parallel to the 1D tube [16].

In this work, we consider the situation that the dipole moment is perpendicular to the 1D tube, where the lowest transverse mode approximation gives a purely repulsive potential (with a $1/z^3$ tail), while our studies reveal effects beyond this approximation. We focus on the low-density limit and discover interesting behaviors of the scattering phase shift to effectively characterize this system. Our main results are summarized as follows.

(i) Instead of a purely repulsive potential, the effective 1D scattering potential is found to contain an attractive part at an interparticle distance of the order of the confinement length. Such a potential induces bound states and gives rise to scattering resonances, which are insensitive to short-range details.

(ii) Because of the $1/z^3$ tail of the dipole potential, the phase shift of the asymptotic two-body wave function at long distance exhibits an unconventional form, as $\cot\delta_k \propto -kD[2\eta + \ln(CkD)]$, where $k$ is the relative momentum, $D$ is the dipole length, $C$ is a constant, and $\eta$ is a dimensionless parameter that incorporates the interplay effect of both the confinement and dipole interaction.

(iii) An asymptotic Bethe ansatz calculation based on the unconventional phase shift shows that, despite the long-range nature of the dipolar interaction, near the resonance region the behavior of spinless bosons is similar to a short-range

*xlcui@iphy.ac.cn

†hzhai@tsinghua.edu.cn

 

Lieb-Liniger gas, which can be simply characterized by a coupling constant.

## II. ONE-DIMENSIONAL EFFECTIVE POTENTIAL

We consider a one-dimensional system along the $\hat{z}$ direction with strong harmonic confinement in the transverse $xy$ plane and the dipole moment $\mathbf{d}$ lies in $xy$ plane perpendicular to the $\hat{z}$ direction, as shown in Fig. 1(a). The Hamiltonian for the relative motion of the two-body problem is given by

$$\left(-\frac{\hbar^2}{2\mu}\nabla^2+\frac{1}{2}\mu\omega^2\rho^2+V(\mathbf{r})\right)\psi(\mathbf{r})=E\psi(\mathbf{r}), \qquad (1)$$

where $\mu=m/2$ is the reduced mass, $\rho=\sqrt{x^2+y^2}$ is the transversal radius, $\omega$ is the frequency of the transverse harmonic potential, and $V(\mathbf{r})=V_{\rm a}(\mathbf{r})+V_{\rm d}(\mathbf{r})$ is shown in Fig. 1(b). Here $V_{\rm a}$ denotes the potential on an atomic scale and $V_{\rm a}(\mathbf{r})$ is chosen as a square-well potential $V_{\rm a}(\mathbf{r})=-V_0$ for $r<r_0$ for simplicity. In addition, $r_0$ is much smaller than the confinement length $a_\perp=\sqrt{\hbar/\mu\omega}$. The dipole part $V_{\rm d}(\mathbf{r})=d^2(1-3\cos^2\xi)/r^3$ for $r>r_0$, where $\xi$ is the angle between $\mathbf{d}$ and $\mathbf{r}$. The dipole length $D=\mu d^2/\hbar^2$ can be tuned to be comparable to or even larger than $a_\perp$.

If we fix $\mathbf{d}$ in the $xy$ plane, say, $\mathbf{d}=d\hat{x}$ (defined as the fixed dipole model), the rotational symmetry around $\hat{z}$ is broken, which makes the numerical calculation quite involved. To reduce the numerical complexity, we first consider a simpler model, in which $\mathbf{d}$ is rapidly rotating around $\hat{z}$ with frequency much larger than any other energy scale in the problem (defined by the rotating dipole model) as considered in Ref. [15]. Upon time averaging, the rotational symmetry around $\hat{z}$ is restored and the effective dipolar interaction becomes $V_{\rm d}=d^2(3\cos^2\theta-1)/2r^3$, where $\theta$ is the angle between $\mathbf{r}$ and $\hat{z}$. With the knowledge obtained from the rotating dipole model, our discussion will later return to the fixed dipole model since it is more realistic.

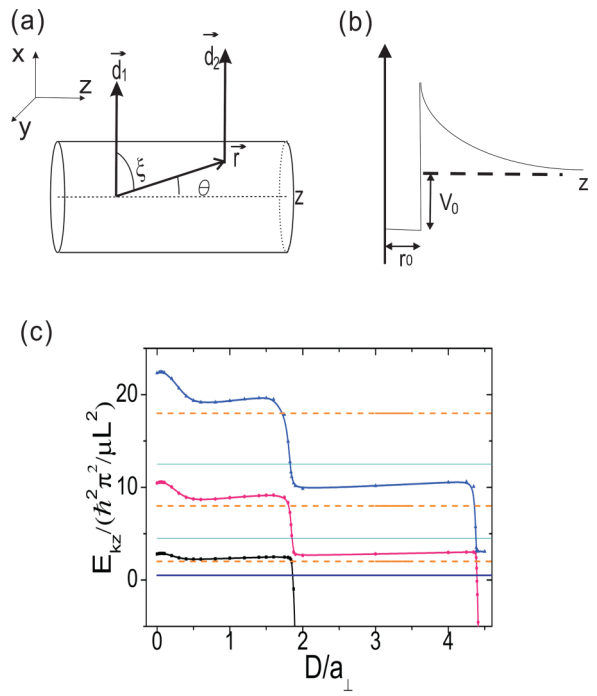


FIG. 1. (Color online) (a) Schematic of our system. (b) Schematic of the two-body interaction potential along $\hat{z}$ with $x=y=0$ fixed. (c) Numerical solution of the lowest eigenstates as a function of $D/a_\perp$. Here $E_{kz}=E-\hbar\omega$ is the kinetic energy in the $z$ direction. We take $r_0=0.1a_\perp$ and $V_0=-136\hbar\omega$ for the short-range square-well potential. The sample size is $L=60a_\perp$ along $z$. The solid horizontal lines are noninteracting energy levels and the dashed horizontal lines are energy levels with phase shift $\pi/2$.

We numerically solve the rotating dipole model with a discrete variable representation [18–20] in a cylindrical box. We consider $s$-wave scattering and the corresponding even-parity eigenstates. Thus, in the rest of this paper we only consider a wave function at $z>0$. The eigenspectrum is plotted as a function of $D/a_\perp$ in Fig. 1(c). We find that as $D/a_\perp$ increases, the energy levels will decrease visibly at a certain window of $D/a_\perp$ and eventually at larger $D/a_\perp$ a series of bound states appears in sequence. We have also found that the positions for the onset of bound states are insensitive to changing $V_0$ with $r_0$ fixed, which only modifies the atomic potential part. Rather, the onsets of bound state are sensitive to changing $r_0$ with $V_0$ fixed, which modifies not only the atomic potential but also the cutoff length scale of the dipole part. This strongly indicates that the bound state originates from the dipolar interaction rather than the potential on an atomic scale.

Therefore, to understand how the dipole interaction could induce bound states, we shall deduce an effective one-dimensional interaction potential $V_{\rm 1d}(z)$. Previously, one commonly used approach was to assume that molecules always stay in the lowest transverse confinement mode $\phi_0(\rho)$ and this single-mode approximation (SMA) gives

$$\begin{aligned}&V_{\rm 1d}^{\rm SMA}\left(\frac{z}{a_\perp}\right)\\&=\int\int dx\,dy\,V_{\rm d}(\mathbf{r})\phi_0^2(\rho)\\&=\frac{\hbar^2}{\mu}\frac{D}{a_\perp^3}\left[\sqrt{\pi}\left(1+2\frac{z^2}{a_\perp^2}\right)e^{z^2/a_\perp^2}\mathrm{erfc}\left(\frac{z}{a_\perp}\right)-2\frac{z}{a_\perp}\right].\end{aligned} \qquad (2)$$

Here the SMA is applied outside the short-range cutoff $r_0$ [21]. As expected, $V_{\rm 1d}^{\rm SMA}(z)$ is a purely repulsive potential and behaves as $(\hbar^2/\mu)D/z^3$ for large $z/a_\perp\gtrsim 1$ and this potential cannot support any bound state. Alternatively, we can deduce $V_{\rm 1d}(z)$ from the numerical solution of the eigenfunction $\psi(\rho,z)$ and eigenvalue $E$ in the following way. Noting that the overall weight of $\psi(\rho,z)$ on the lowest transverse mode $\phi_0(\rho)$ is nearly unity in a quite wide range of $z/a_\perp$ [see the inset of Fig. 2(a)], we can therefore define a projected 1D wave function $\psi_{\rm 1d}(z)=\int dx\,dy\,\phi_0(\rho)\psi(\rho,z)$. Assuming that $\psi_{\rm 1d}(z)$ satisfies a 1D Schrödinger equation $[-(\hbar^2/2\mu)d^2/dz^2+V_{\rm 1d}(z)]\psi_{\rm 1d}(z)=(E-\hbar\omega)\psi_{\rm 1d}(z)$, we obtain $V_{\rm 1d}$ as

$$V_{\rm 1d}(z)=\frac{\hbar^2}{2\mu}\frac{\frac{d^2}{dz^2}\psi_{\rm 1D}(z)}{\psi_{\rm 1D}(z)}+E-\hbar\omega, \qquad (3)$$

In Fig. 2(a) we compare $V_{\rm 1d}$ with $V_{\rm 1d}^{\rm SMA}$ and find that in the region $z/a_\perp\gtrsim 1$ these two potentials agree very well, whereas at a short distance when $z/a_\perp\lesssim 1$, $V_{\rm 1d}$ starts to deviate from $V_{\rm 1d}^{\rm SMA}$ and finally $V_{\rm 1d}$ becomes attractive. This is because the dipole interaction increases strongly at a short distance and

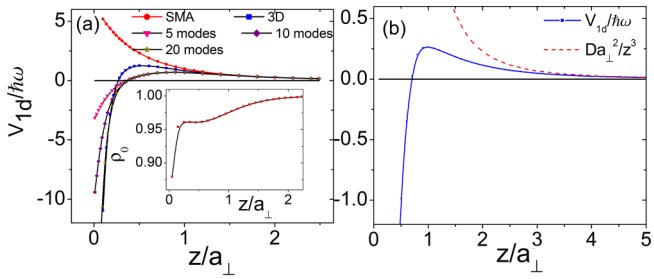


FIG. 2. (Color online) Effective potential for the (a) rotating dipole model and (b) fixed dipole model at $D/a_\perp = 1.825$. The inset of (a) shows the weight of $\psi(\rho,z)$ on the lowest transverse mode, i.e., $\rho_0 = \frac{|\psi_{1d}(z)|^2}{\int|\psi(\rho,z)|^2 d^2\rho}$. Different lines in (a) correspond to the SMA and MMA with 5, 10, and 20 modes included, and the full three-dimensional numerical results. In (b) the blue solid line corresponds to the MMA with 10 modes and the dashed line corresponds to the $D/z^3$ potential.

can overcome the confinement potential and the higher-order scattering processes via higher transverse modes give rise to attraction. The enhanced short-range attraction with increasing $D/a_\perp$ reduces energies of scattering states and finally leads to bound states, as shown previously in Fig. 1(c). In particular, when a bound state starts to emerge near the threshold, the low-energy scattering behavior will be dramatically modified and $V_{1d}^{SMA}$ fails to describe the low-energy physics.

Nevertheless, the SMA can be improved by including higher transverse modes. Considering $\hat{H}_\rho = -\frac{\hbar^2}{2\mu}(\partial_x^2+\partial_y^2) + \frac{1}{2}\mu\omega^2\rho^2 + V(\mathbf{r})$ and expanding $\hat{H}_\rho$ in the harmonic oscillator eigenbasis $\phi_i(\rho)$ as $H_\rho^{ij}(z) = \int dx\,dy\,\phi_i(\rho)\hat{H}_\rho\phi_j(\rho)$, the matrix $H_\rho(z)$ can be diagonalized by a unitary transformation $X^\dagger(z)H_\rho(z)X(z) = \Lambda(z)$. Using an adiabatic approximation [10], the multimode approach (MMA) gives an effective potential $V_{1d}^{MMA}(z) = \Lambda^{00}(z)$. In Fig. 2(a) we also compare $V_{1d}^{MMA}(z)$ with $V_{1d}$ and we find that $V_{1d}^{MMA}(z)$ can reproduce the short-range attraction reasonably well, as long as one keeps sufficient modes. Therefore, we conclude that the MMA provides the correct physical understanding for the 1D effective potential. As the underlying physics of the MMA is so generic, it can also be applied to the fixed dipole model. An effective potential for the fixed dipole model is obtained as shown in Fig. 2(b) with the MMA. Similar to the rotating dipole model, it coincides with $D/z^3$ when $z \gtrsim a_\perp$ and gradually becomes attractive when $z \lesssim a_\perp$. The following discussion is based on such an effective 1D potential, which can be applied to both two models.

## III. LOW-ENERGY PHASE SHIFT

When $z \gtrsim a_\perp$, the wave functions can be solved perturbatively in two different regions. In region I, $z \gg D$, and in region II, $z \ll 1/k$. The wave function for $z \lesssim a_\perp$, where the potential deviates from $D/z^3$, will not be studied explicitly; instead, it determines the boundary condition for region II.

In region I, we take $\psi_I(z) = A_k[\cot\delta_k W(kz) - V(kz)]$, where $A_k$ is a normalization factor and $W(kz)$ and $V(kz)$ are two independent solutions that can be expanded as $W(kz) = \sum_n (kD)^n W_n(kz)$ and $V(kz) = \sum_n (kD)^n V_n(kz)$ when the $D/z^3$ term is treated as a perturbation for $z \gg D$. To zeroth order we have $\psi_I(z) \propto \cos(kz+\delta_k)$ and thus $W_0(kz) = \cos(kz)$ and $V_0(kz) = \sin(kz)$, where $\delta_k$ is the phase shift. To the next order, we find $W_1(\xi)$ and $V_1(\xi)$ ($\xi$ denotes $kz$) as

$$W_1(\xi) = -\mathrm{Ci}(2\xi)\sin\xi + \frac{1}{2}\cos\xi\left[\frac{1}{\xi} + 2\,\mathrm{Si}(2\xi) - \pi\right],$$
$$V_1(\xi) = -\mathrm{Ci}(2\xi)\cos\xi + \frac{1}{2}\sin\xi\left[\frac{1}{\xi} - 2\,\mathrm{Si}(2\xi) + \pi\right], \quad (4)$$

where $\mathrm{Ci}(z) = -\int_z^\infty \frac{\cos t}{t}dt$ and $\mathrm{Si}(z) = \int_0^z \frac{\sin t}{t}dt$. Up to $O(\xi)$, by expanding $\psi_I(z)$ in terms of $\xi$, we have

$$\psi_I(z) = A_k\Big(\cot\delta_k - kD\frac{z}{D} - \frac{kD}{2}\cot\delta_k\{1-2\gamma_E - 2[\ln(2kD)+\ln(2z/D)]\}\Big), \quad (5)$$

where $\gamma_E$ is Euler's constant.

In region II, when $z \ll 1/k$, we can treat the $k^2\psi(z)$ term as a perturbation. To $O(kz)$, we only need to consider the zero-energy solutions of the $D/z^3$ potential, with the general form given by

$$\psi_{II}(z) = \sqrt{z/D}[K_1(2\sqrt{D/z}) + \eta I_1(2\sqrt{D/z})], \quad (6)$$

where $K_1$ and $I_1$ are, respectively, the regular and irregular solutions for the $D/z^3$ potential. Their relative coefficient $\eta$ is determined by potential details at short range, which can be tuned by $D/a_\perp$ in the present model (see the inset of Fig. 4). In the following discussion of low-energy physics, $\eta$ serves as an independent input parameter, which describes the effect of the short-range potential on the long-range physics. If the potential is close to a pure $D/z^3$ potential, $\eta \to 0$; if the short-range part is about to form a bound state, $\eta \to +\infty$; and if a bound state has been formed near the threshold, $\eta \to -\infty$. By expanding $\psi_{II}(z)$ at large $z/D$, one obtains

$$\psi_{II}(z) = \frac{z}{2D} - \frac{\ln(z/D)}{2} + \eta + \gamma_E - \frac{1}{2} + O(D/z). \quad (7)$$

Finally, for low-energy scattering $kD \ll 1$, we require $\psi_I(z)$ of Eq. (5) and $\psi_{II}(z)$ of Eq. (7) to behave in the same way in their overlap region $D \ll z \ll 1/k$. Thus, by equating the relative coefficients of $z/D$, $\ln(z/D)$, and constant terms between Eqs. (5) and (7), we can obtain two coupled equations for $A_k$ and $\cot\delta_k$, the solution of which gives the low-energy behavior of the phase shift

$$\cot\delta_k = -kD[2\eta + \ln(CkD)], \quad C = 2e^{3\gamma_E - 3/2}. \quad (8)$$

To verify this phase shift we numerically solve the 1D Schrödingier equation with a boundary condition at short distance $z^*$ ($\ll D$). In this case, the boundary condition can be satisfied by a given $\eta$ for the zero-energy solution. From the numerical solution we can extract $\delta_k$ from the asymptotic two-body wave function behavior at a large distance. We plot $\cot\delta_k$ as a function of $kD$ and compare it with the formula 8) in Fig. 3 and find that they agree reasonably well for sufficient low energies [22]. The logarithmic correction reflects the long-range nature of the dipole interaction.

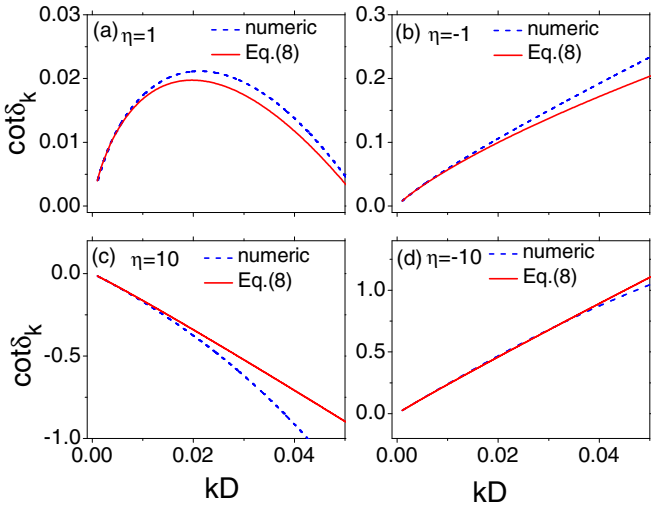


FIG. 3. (Color online) Plot of $\cot\delta_k$ determined by numerics (blue dashed lines) compared with the analytical formula (8) (red solid lines) for (a) $\eta = 1$, (b) $\eta = -1$, (c) $\eta = 10$, and (d) $\eta = -10$.

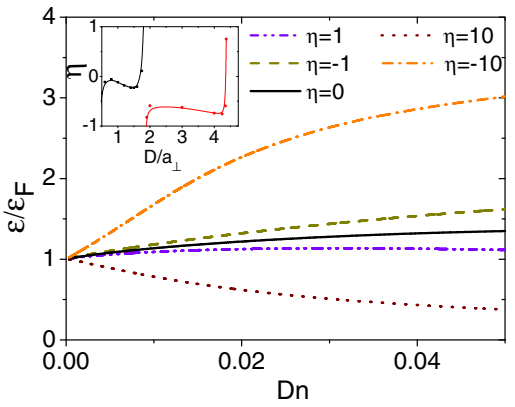


FIG. 4. (Color online) Energy density of spinless bosons as a function of $Dn$ for different $\eta$. Here $n$ is the density of 1D bosons, $\mathcal{E}_F$ is the energy density for identical fermions with the same density, and $\eta$ can be tuned by $D/a_\perp$ in the quasi-1D model, as shown in the inset.

## IV. MANY-BODY SYSTEM OF SPINLESS BOSONS

Hereafter we study a many-body system of spinless dipolar bosons with an asymptotic Bethe ansatz [23]. The asymptotic Bethe ansatz only makes use of the scattering phase shift to obtain the thermodynamics of a system with finite density. Following the standard procedure [23], we obtain $k_j L = 2\pi I_j - 2\sum_{i\neq j}\delta((k_j - k_i)/2)$, where $I_j$ are quantum numbers and $\delta(k)$ is the two-body phase shift obtained in Eq. (8). In the thermodynamic limit one obtains a Fredholm-type equation

$$\rho(k) = \frac{1}{2\pi} + \frac{1}{\pi}\int_{-B}^{B} \frac{\partial\delta\left(\frac{k-q}{2}\right)}{\partial k}\rho(q)dq. \tag{9}$$

The density and the energy density are, respectively,

$$n = \int_{-B}^{B}\rho(k)dk, \quad \mathcal{E} = \int_{-B}^{B}k^2\rho(k)dk. \tag{10}$$

The solution of Eqs. (9) and (10) gives $\mathcal{E}/\mathcal{E}_F$ as a function of $Dn$ for different $\eta$, with $\mathcal{E}_F$ the energy density for identical fermions with the same density. In Fig. 4 we display how the energy density behaves across a resonance.

We find for all $\eta$ that the energy density approaches the Tonks limit, i.e., $\mathcal{E}/\mathcal{E}_F \to 1$, in the dilute limit of $Dn \to 0$, because the phase shift $\delta_k \to \pi/2$ when $k \to 0$. Near a resonance when $|\eta|$ is sufficiently large, as long as $kD \gg e^{-|\eta|}$, the $2\eta$ term dominates over the logarithmic term in Eq. (8) and the phase shift can be well approximated as $\cot\delta_k = -kD\eta$. This gives a nearly-energy-independent interaction constant $g_{1d} = \hbar^2/\mu D\eta$ and the interaction parameter $\gamma = 1/\eta nD$. Here $\gamma$ decreases with $D$ for $\eta > 0$ and increases for $\eta < 0$. As shown in Fig. 4, for positive $\eta$, the energy density $\mathcal{E}$ decreases as $D$ increases, similar to the usual Lieb-Liniger gas [24]; for negative $\eta$, this system is in the super-Tonks region and $\mathcal{E}$ increases with $D$ [25]. Finally, once away from resonance, when $|\eta|$ is small, the logarithmic term dominates over the $2\eta$ term in Eq. (8) as long as $kD \ll 1$. In this region, the physics cannot be analogous to that with a zero-range interaction since the logarithmic term prevents defining an energy-independent interaction constant. In this region, we numerically find that the energy density almost stays static around $\mathcal{E}_F$ with varying $Dn$.

## V. CONCLUSION

Our discussion here can be straightforwardly generalized to the quasi-2D case, where the dipole moment is perpendicular to the 2D plane. A previous study of this system pointed out a similar behavior as a short-range attraction of the effective potential [26]. However, it was also observed that the induced scattering resonances in quasi two dimensions is extremely narrow [27] in comparison to the quasi-1D case discussed in this paper. This is because it is naturally more difficult to form a bound state in two dimensions than in one dimension for a given potential (here with both repulsive and attractive parts), as the kinetic energy cost (at short range) of a bound state is higher in higher dimensions. As a result, it requires a larger dipole moment $D$ to generate strong enough short-range attraction for scattering resonances. In turn, the larger $D$ enhances the repulsive barrier at an intermediate distance of two dipoles and makes the coupling between the scattering state and bound state much weaker [28]. That is to say, the irregular part of the wave function is not important except for a very narrow range of the dipole moment. A pure $1/\rho^3$ repulsive potential works much better in two dimensions compared to the 1D case discussed in this paper.

## ACKNOWLEDGMENTS

We thank Gora Shlyapnikov, Peng Zhang, and Zhe-Yu Shi for useful discussion. This work was supported by Tsinghua University Initiative Scientific Research Program, NSFC under Grants No. 11104158 (X.C.), No. 11104157(R.Q.), No. 11004118 (H.Z.), and No. 11174176 (H.Z.) and NKBRSFC under Grant No. 2011CB921500.

[1] K.-K. Ni, S. Ospelkaus, M. G. H. de Miranda, A. Peer, B. Neyenhuis, J. J. Zirbel, S. Kotochigova, P. S. Julienne, D. S. Jin, and J. Ye, Science **322**, 231 (2008); S. Ospelkaus, K.-K. Ni, G. Quemener, B. Neyenhuis, D. Wang, M. H. G. de Miranda, J. L. Bohn, J. Ye, and D. S. Jin, Phys. Rev. Lett. **104**, 030402 (2010).

[2] P. S. Zuchowski and J. M. Hutson, Phys. Rev. A **81**, 060703(R) (2010).

[3] S. Tan, Ann. Phys. (NY) **323**, 2952 (2008); **323**, 2971 (2008).

[4] M. Olshanii, Phys. Rev. Lett. **81**, 938 (1998).

[5] E. Haller, M. Gustavsson, M. J. Mark, J. G. Danzl, R. Hart, G. Pupillo, and H. Nagerl, Science **325**, 1224 (2009).

[6] M. Marinescu and L. You, Phys. Rev. Lett. **81**, 4596 (1998); B. Deb and L. You, Phys. Rev. A **68**, 033408 (2003).

[7] C. Ticknor and J. L. Bohn, Phys. Rev. A **72**, 032717 (2005).

[8] K. Kanjilal and D. Blume, Phys. Rev. A **78**, 040703(R) (2008).

[9] V. Roudnev and M. Cavagnero, J. Phys. B **42**, 044017 (2009); Phys. Rev. A **79**, 014701 (2009).

[10] Z. Y. Shi, R. Qi, and H. Zhai, Phy. Rev. A **85**, 020702(R) (2012).

[11] R. Qi, Z. Y. Shi, and H. Zhai, Phys. Rev. Lett. **110**, 045302 (2013).

[12] T. Shi, S. H. Zou, H. Hu, C.-P. Sun, and S. Yi, Phys. Rev. Lett. **110**, 045301 (2013).

[13] F. Deuretzbacher, J. C. Cremon, and S. M. Reimann, Phys. Rev. A **81**, 063616 (2010); **87**, 039903(E) (2013).

[14] N. T. Zinner, B. Wunsch, I. B. Mekhov, S.-J. Huang, D.-W. Wang, and E. Demler, Phys. Rev. A **84**, 063606 (2011); M. D. Girardeau and G. E. Astrakharchik, Phys. Rev. Lett. **109**, 235305 (2012); A. G. Volosniev, J. R. Armstrong, D. V. Fedorov, A. S. Jensen, M. Valiente, and N. T. Zinner, New J. Phys. **15**, 043046 (2013); F. Deuretzbacher, G. M. Bruun, C. J. Pethick, M. Jona-Lasinio, S. M. Reimann, and L. Santos, Phys. Rev. A **88**, 033611 (2013).

[15] S. Sinha and L. Santos, Phys. Rev. Lett. **99**, 140406 (2007).

[16] P. Giannakeas, V. S. Melezhik, and P. Schmelcher, Phys. Rev. Lett. **111**, 183201 (2013).

[17] N. Bartolo, D. J. Papoular, L. Barbiero, C. Menotti, and A. Recati, Phys. Rev. A **88**, 023603 (2013).

[18] D. Baye and P.-H. Heenen, J. Phys. A: Math. Gen. **19**, 2041 (1986).

[19] V. Szalay, J. Chem. Phys. **99**, 1978 (1993).

[20] E. Tiesinga, C. J. Williams, F. H. Mies, and P. S. Julienne, Phys. Rev. A **61**, 063416 (2000).

[21] The SMA gives a residual $\delta(z)$ term when the dipole potential extends to the scattering center $r = 0$ [13,15,17]. However, in a realistic system the short-range physics is dominated by the van der Waals potential (in our case it is modeled by a square-well potential), with typical range $r_0$, rather than the dipole potential. Therefore, we consider such an extension of the dipole potential to $r < r_0$ unrealistic and the result of a $\delta$ term an artificial outcome.

[22] We find an empirical fitting formula for the phase shift $\cot\delta_k = -kD\{2 + (1/\eta)[\ln(CkD)]\}/[1/\eta + b(kD)^2\ln(kD)]$, which fits the numerical results in a wider energy range, in particular, in the region when $\eta$ is large. Here $b$ is a fitting constant. For small $\eta$ or small $k$, this formula is consistent with Eq. (8).

[23] B. Sutherland, Phys. Rev. Lett. **75**, 1248 (1995); B. Sutherland, *Beautiful Models* (World Scientific, Singapore, 2004); E. Gutkin, Ann. Phys. (NY) **176**, 22 (1987); J. Y. Lee, X.-W. Guan, A. del Campo, and M. T. Batchelor, Phys. Rev. A **85**, 013629 (2012).

[24] E. H. Lieb and W. Liniger, Phys. Rev. **130**, 1605 (1963).

[25] G. E. Astrakharchik, J. Boronat, J. Casulleras, and S. Giorgini, Phys. Rev. Lett. **95**, 190407 (2005).

[26] C. Ticknor, Phys. Rev. A **81**, 042708 (2010).

[27] J. P. D'Incao and C. H. Greene, Phys. Rev. A **83**, 030702(R) (2011).

[28] Z. Y. Shi (private communication).